Nonlinear Analysis of Active Vibration Absorber as a Wearable Rest Tremor Suppression in Parkinson's Disease

S. Mohanty and S. K. Dwivedy

1 Introduction

The involuntary movement disorders of Parkinson's disease (PD) patient causing tremors in the forearm, wrist, neck, complete hand, and other different body parts are increasing globally, more especially in the developed countries [1, 2]. In India, the population of tremors-based PD patient is around 25 per 1 lakh people but in countries like USA, Singapore, and Paris tremors PD patients are 237 per 1 lakh people [3]. Globally, more than 4% of the population over 40 years suffer from tremors [4]. The most common targets of tremors in PD patients are on the hand and neck portions. Tremors in PD patients are related to neurological disorders and often very difficult to treat the patient completely with medication and surgery. Therefore, many mechanical-based attachments are developed to suppress the constant vibration of the forearm and wrist of the PD patients. There are five types of tremors, namely resting tremors, action tremors, postural tremors, intention tremors, and task-specific tremors, which vibrate certain part of the body at a frequency range of 3–6 Hz [4, 5]. Among these resting tremors are more common which falls under the category of essential tremors. Many studies have been undertaken both experimentally and theoretically to develop wearable device [6] which can suppress the vibration of the tremors patient. Hashemi et al. [7] theoretically and experimentally investigated and evaluated the optimum distance of the tuned vibration absorber to suppress 80% of tremors in PD patients. Gebai et al. [8, 9] parametrically studied many enhanced passive tuned mass dampers to suppress the tremors in the wrist, forehand, and shoulder of the PD patient. Buki et al. [4] designed and developed a passive dynamic vibration absorber via a bracelet model using fixed-point optimization technique to suppress 85% of vibration of forearm tremors. López-Blanco et al. [10] designed

S. Mohanty (✉) · S. K. Dwivedy
Department of Mechanical Engineering, Indian Institute of Technology Guwahati, Guwahati, Assam 781039, India

D. Maity et al. (eds.), *Recent Advances in Computational and Experimental Mechanics, Vol–I*, Lecture Notes in Mechanical Engineering,
https://doi.org/10.1007/978-981-16-6738-1_53

and tested gyroscope integrated smartwatches on the tremor in Parkinson's disease patients and showed good acceptance among the patients. Habib et al. [11] achieved minimum vibration of the nonlinear SDOF main structure under harmonic excitation by a nonlinear passive vibration absorber by obtaining optimal stiffness and damping ratio parameters, which can be used to suppress tremors in PD patients. Mohanty and Dwivedy [12–16] used active vibration absorber to suppress vibration of the nonlinear system for various resonance conditions. From the above literature, it is observed that nonlinear analysis of forearm tremors and active force is not explored more. Hence, in the present analysis, these cases are taken into consideration. The mathematical modeling of the system is given below.

2 Mathematical Modeling

In Fig. 1, the main vibrating structure is modeled as the forearm of a PD patient with pertinent inertia for pronation/supination tremor around its longitudinal axis. The forearm is shown in Fig. 1 and is modeled as a nonlinear SDOF main structure with a mass (M), linear spring (K), nonlinear spring (K_3), and a damper (C) with base vibration. The main structure is also subjected to external harmonic forcing excitation of $F_1 \cos(\Omega t)$. The reduction of vibration of the forearm is achieved by attaching an active nonlinear vibration absorber to the main structure. The active nonlinear vibration absorber model consists of a mass (m), linear spring (k), nonlinear spring (k_3), damper (c), and an actuator. The active force (F_{c1}) by the actuator is produced by considering acceleration feedback from the main structure, which is equal to $k_c\ddot{x}_1$, where k_c is the control gain. Here, x_0, x_1, and x_2 indicate the displacement of the base, the main structure, and the vibration absorber, respectively (Fig. 1). The dynamics of the system are represented by two coupled nonlinear ordinary differential equations of motion which are given below.

$$\begin{aligned} M\ddot{x}_1 &= K(x_0 - x_1) + C(\dot{x}_0 - \dot{x}_1) + k(x_2 - x_1) + c(\dot{x}_2 - \dot{x}_1) \\ &\quad -K_3(x_0 - x_1)^3 + k_3(x_2 - x_1)^3 + F_1 \cos(\Omega t) - F_{c1} \end{aligned} \tag{1}$$

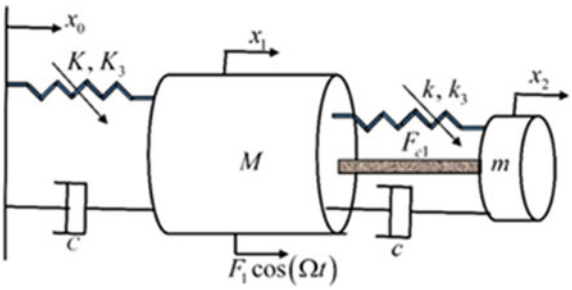

Fig. 1 Nonlinear active vibration absorber attached to the nonlinear main structure

$$m\ddot{x}_2 = c_2(\dot{x}_1 - \dot{x}_2) + k_2(x_1 - x_2) + k_3(x_1 - x_2)^3 + F_{c1} \tag{2}$$

.

It may be noted that the exclusion of controlling force F_{c1}, nonlinear spring stiffness of the main structure K_3, nonlinear spring stiffness in the absorber k_3, and external harmonic force excitation $F_1 \cos(\Omega t)$, Eqns. (1) and (2) can be reduced to that of Buki et al. [4]. The governing Eqs. (1) and (2) are modified by assuming $\omega_1 = \sqrt{K/M}$.

$$\begin{aligned}\ddot{x}_1 &= \omega_1^2(x_0 - x_1) + 2\xi_1\omega_1(\dot{x}_0 - \dot{x}_1) + \mu\omega_2^2(x_2 - x_1) + 2\mu\xi_2\omega_2(\dot{x}_2 - \dot{x}_1) \\ &+\alpha(x_0 - x_1)^3 + \mu\beta(x_2 - x_1)^3 + F\cos\Omega t - F_c\end{aligned} \tag{3}$$

$$\ddot{x}_2 = 2\xi_2\omega_2(\dot{x}_1 - \dot{x}_2) + \omega_2^2(x_1 - x_2) + \beta(x_1 - x_2)^3 + F_c \tag{4}$$

where

$$\mu = \frac{m}{M},\ \xi_1 = \frac{C}{2\sqrt{KM}},\ \xi_2 = \frac{c}{2\sqrt{km}},\ \alpha = \frac{K_3}{M},\ \beta = \frac{k_3}{m},\ F = \frac{F_1}{M},\ F_c = \frac{F_{c1}}{M},\ \omega_2 = \sqrt{k/m}$$

The approximate solution of the Eqs. (3) and (4) is solved using the HBM and described in the next section.

2.1 Solution Obtained by HBM

In the present section, the approximate steady-state solution of Eqs. (3) and (4) is solved by HBM by assuming the solution as follows.

$$x_0 - x_1 = a_1(t)\cos(\Omega t - \theta_1(t)) \tag{5}$$

$$x_1 - x_2 = a_2(t)\cos(\Omega t - \theta_2(t)) \tag{6}$$

Here, $a_1(t)$, $\theta_1(t)$, $a_2(t)$, and $\theta_2(t)$ are functions of time t in a way that the following higher order terms: $\ddot{a}_1$, $\ddot{\theta}_1$, $\ddot{a}_2$, $\ddot{\theta}_2$, $\dot{a}_1\dot{\theta}_1$, $\dot{a}_2\dot{\theta}_2$, $\dot{\theta}_1^2$, and $\dot{\theta}_2^2$ can be neglected. Substituting Eqs. (5) and (6) into Eqs. (3) and (4), one can obtain four sets of equations consisting sin Ωt and cos Ωt terms. From these four sets of equations, the coefficients of sin Ωt and cos Ωt terms are collected which are represented in a compact matrix form and shown below.

$$\underbrace{\begin{bmatrix} a_{11} & a_{12} & a_{13} & a_{14} \\ a_{21} & a_{22} & a_{23} & a_{24} \\ a_{31} & a_{32} & a_{33} & a_{34} \\ a_{41} & a_{42} & a_{43} & a_{44} \end{bmatrix}}_{A} \underbrace{\begin{Bmatrix} \dot{a}_1 \\ \dot{\theta}_1 \\ \dot{a}_2 \\ \dot{\theta}_2 \end{Bmatrix}}_{\dot{X}} = \underbrace{\begin{Bmatrix} b_1 \\ b_2 \\ b_3 \\ b_4 \end{Bmatrix}}_{B} \tag{7}$$

From Eq. (7), the steady-state amplitude and phase equations are obtained as follows.

$$\left[\dot{X}\right] = [A]^{-1}[B] \tag{8}$$

The steady-state solutions are obtained from the reduced Eq. (8) by taking $\dot{a}_1 = \dot{\theta}_1 = \dot{a}_2 = \dot{\theta}_2 = 0$. These steady-state solutions are then solved by using Newton's method to study the responses of the system which are discussed in the next section. It may be noted that the above method is similar to the authors' previous work [12].

3 Result and Discussions

In the present portion, the potential of the NAVA in vibration suppression of the nonlinear SDOF main structure/forearm is studied by the frequency responses, time responses, phase portraits, and Poincare sections for various system parameters such as nonlinear stiffness, active force, the single and multi-harmonic force of excitation on the main structure. The frequency response curves of the main structure and the active nonlinear absorber are found out by numerically solving the steady-state equations from Eq. 8 by using Newton's method. The efficacy of active force and cubic nonlinear spring stiffness is studied by comparing with [4]. The mass, linear stiffness, and damping parameters of the main forearm structure and the bracelet are considered from the work of Buki et al. [4] which are given below. The mass ratio between the bracelet/absorber and the forearm/main structure is considered equal to $\mu = m/M = 0.2$, damping ratio of the forearm $\xi_{\text{Arm}} = C/2\sqrt{KM} = 0.079$, damping ratio of the absorber $\xi_{\text{Absorber}} = c/2\sqrt{\text{km}} = 0.0264$, the mass of the absorber 0.28 kg, the mass of the forearm for a 60 kg person 1.122 kg, natural frequency of the forearm 4.56 Hz, natural frequency of the absorber/bracelet 5.85 Hz. The external harmonic forcing amplitude is considered equal to $F = 0.1$ N/kg.

In Sects. 3.1 and 3.2, frequency responses are studied for the linear and nonlinear system by with and without active force. These results are compared with the published literature. In subsections 3.3 to 3.5, time responses, phase portraits, and Poincare sections of the system are studied when the forearm is subjected to single and multi-excitation forces. In the following subsection, the frequency response of the passive linear and nonlinear system is studied.

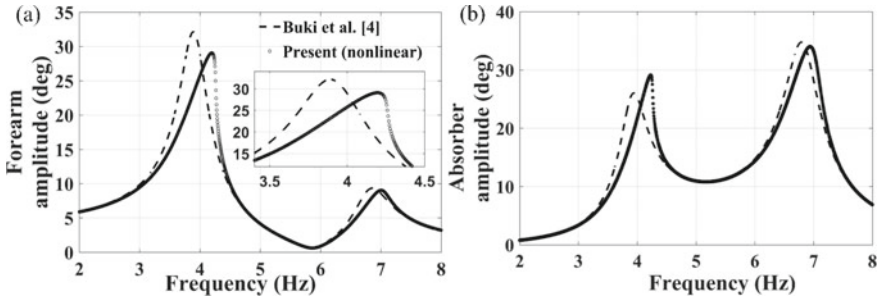

Fig. 2 Frequency response of the linear and nonlinear system **a** forearm, **b** bracelet

3.1 Frequency Responses with Variation in Cubic Nonlinear Stiffness

The frequency response curves of the forearm and the bracelet with and without cubic nonlinear stiffness in the bracelet are shown in Fig. 2 with the same system parameters as in [4]. The cubic nonlinear stiffness coefficient for the bracelet is considered to be 5% of the linear stiffness. From Fig. 2a, it can be observed that considering cubic nonlinear stiffness in the bracelet, the response amplitude of the forearm decreases 10% at the peaks, and also for a small range between 3 and 4 Hz compared to the linear vibration absorber reported in [4]. However, from Fig. 2b, it can be noticed that the consideration of cubic nonlinear stiffness in the bracelet increases the response than the linear stiffness. It is inferred from Fig. 2 that with nonlinear cubic stiffness, the response amplitude of the forearm decreases. But, for a higher nonlinear stiffness coefficient, the response becomes unstable near the first peak. Hence, the nonlinear stiffness coefficient should be within 5% of linear stiffness to reduce the vibration of the forearm due to tremor.

3.2 Effects of Active Force and Optimal Design Parameters on the Frequency Responses

The comparison of tremor suppression of the forearm for various system parameters such as with and without the active control force, without absorber, and with optimal active absorber is shown in Fig. 3. From Fig. 3a, it can be noted that the maximum response amplitude of the forearm reduces to 85% at the peak, and also from 4 to 6 Hz, the response amplitude decreases compared to without absorber which is well matched from the work of [4]. From the present work, with the active force of 0.05 control gain shifts the peaks of the amplitudes in the forearm and for a broader range of frequencies (3.5–8 Hz), the response amplitude of the forearm is less than [4]. It is also noticed that with the active feedback force, vibrational suppression in the forearm

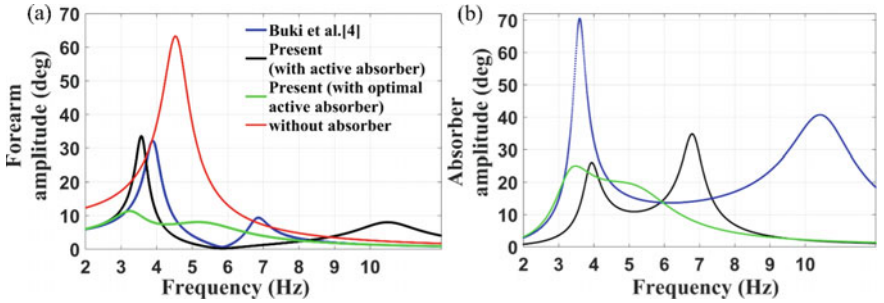

Fig. 3 Frequency responses of the passive and active system **a** forearm, **b** bracelet

reduces 18% at the first peak and 62% at the second peak than the passive absorber [4] at the corresponding operating frequency. Also considering the optimal stiffness in the linear spring, nonlinear spring, and damping ratio in the bracelet/absorber from the formulae derived by Habib et al. [11] and with the optimal active control force as in Ref. 12, the maximum response amplitude of the forearm reduces to 76% than the work of Buki et al. [4]. From Fig. 3b, it may also observe that the response amplitude of the bracelet decreases with the active force.

3.3 Effects of Active Force on the Time Responses

In Fig. 4, the time responses and phase portraits of the forearm and the bracelet are shown by with (blue) and without (black) the active force at the resonating frequency considering nonlinear stiffness in the system. The time responses curves in Fig. 4a show that with the active force, a 77% reduction in the response amplitude of the forearm is achieved than the passive system. However, for the bracelet, it increases by 10% as shown in Fig. 4c. The forearm and the bracelet show periodic and stable characteristics as observed from Fig. 4c, d.

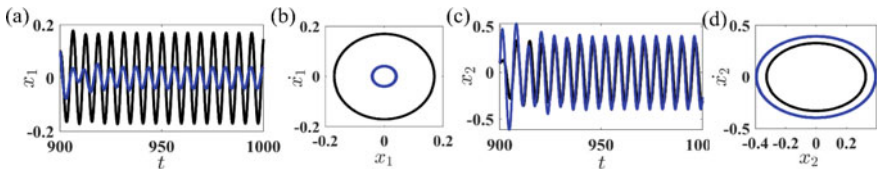

Fig. 4 Time responses and phase portraits for single external harmonic excitation on the forearm **a**–**b** forearm **c**, **d** bracelet, where (with active force and without active force)

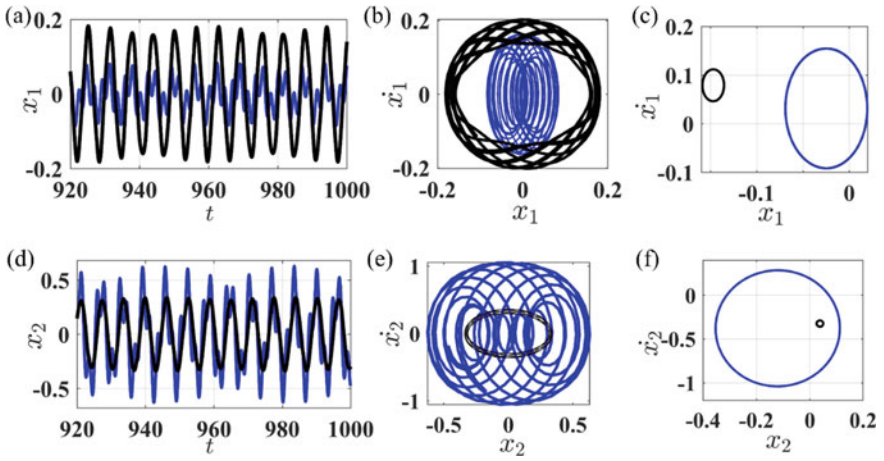

Fig. 5 Time responses, phase portraits, and Poincare sections for two external harmonic excitations on the forearm **a**–**c** forearm **d**–**f** bracelet (with active force and without active force)

3.4 Effects of Active Force on the Time Responses for Two Excitation Forces

In this section, the time responses, phase portraits, and Poincare sections of the system are shown in Fig. 5 for the active and passive cases when the forearm undergoes two external harmonic excitations $F\cos(\Omega t)$ and $F\cos(2\sqrt{2}\Omega t)$. From Fig. 5a, one can observe that with the active force 64% of vibration reduces in the forearm but induces many harmonics and show quasiperiodic response as shown in Fig. 5b, c. However, the response amplitude of the bracelet increases by 44% with the active force as shown in Fig. 5c. The system in both the active and passive cases shows quasiperiodic responses as shown in Fig. 5e, f.

3.5 Effects of Active Force on the Time Responses for Multi-Excitation Forces

In this section, the effect of active force by the bracelet is studied in Fig. 6 when the main structure/forearm undergoes multi external harmonic excitation forces, namely $F\cos(\Omega t)$, $F\cos(2\Omega t)$, $F\cos(4\Omega t)$, $F\cos(8\Omega t)$, and $F\cos(16\Omega t)$. It is observed from Fig. 6a that with the active force 50% of the vibration suppression in the forearm is achieved. However, with the active feedback force, the response of the system is prone to induce more harmonics in the time responses and undergoes chaotic behavior as evident from the phase portraits and Poincare sections which are shown in Fig. 6b, c, respectively, but without the active force, the system shows periodic response. The response of the system for the absorber/bracelet is shown in Fig. 6d, where one can

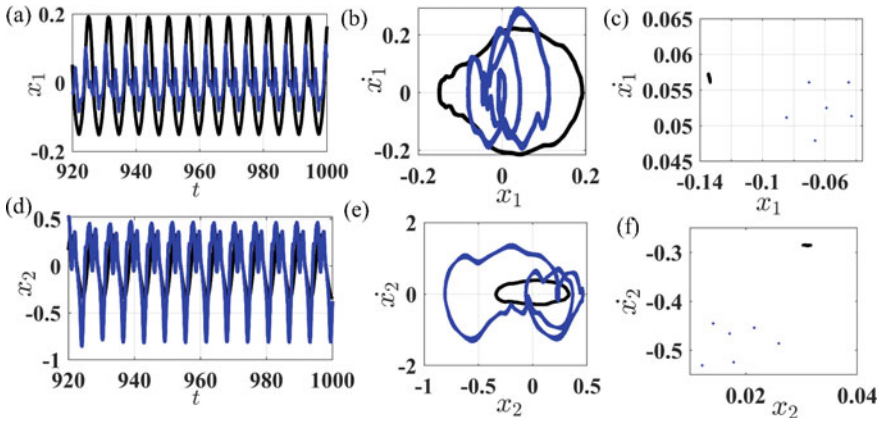

Fig. 6 Time responses, phase portraits, and Poincare sections for multiple external harmonic excitations on the forearm **a–c** forearm **d–f** bracelet (with active force and without active force)

observe 32% increase in the response amplitude of the bracelet with the active force. The phase portraits and Poincare sections of the absorber/bracelet which are shown in Fig. 6e, f and also show similar characteristics as the main structure.

4 Conclusions

In the present analysis, a nonlinear active vibration absorber as a bracelet is modeled to attenuate supination/pronation tremor in the forearm. The proposed model is an extension study of Buki et al. [4], where passive linear vibration absorber is used to suppress tremors in the forearm. From the present analysis, it is inferred that with nonlinear stiffness in the forearm and the bracelet 10% of tremor reduces at the first resonating peak. Moreover, the consideration of nonlinear stiffness in the forearm is more practical. However, the cubic nonlinear stiffness of more than 5% of linear stiffness makes the system unstable. The active feedback force by the actuator attenuates 18% and 62% at the first and second resonating peaks in the frequency response curves of the forearm than the passive vibration absorber from the work of [4]. It is also observed that with the optimal parameters for the bracelet [11] and with active force 90% of the vibration in the forearm are reduced than the recent work of Buki et al. [4]. It may be noted that the optimal damping force for the bracelet is 20% less than the damping used in the work of Buki et al. [4], which is easier to implement. The active force not only suppresses the tremor for a broader range of operating frequencies in the forearm but also significantly attenuates the vibration of the bracelet. The time responses, phase portraits, and the Poincare sections show the effectiveness of the actuator in suppressing the tremor, when the forearm is assumed to undergo single, two, and multi-excitation forces. However, it is also observed

that for multi-excitation forces with the active force, the response shows chaotic responses and quasiperiodic responses.

References

1. Kamble N, Pal PK (2018) Tremor syndromes: a review. Neurol India 66(7):36–47
2. Gourie-Devi M (2014) Epidemiology of neurological disorders in India: review of background, prevalence and incidence of epilepsy, stroke. Parkinson's disease and tremors. Neurol India 62(6):588–598
3. Anouti A, Koller W (1998) Tremor disorders: diagnosis and management. West J Med 162(6):523–530
4. Buki E, Katz R, Zacksenhouse M, Schlesinger I (2018) Vib-bracelet: a passive absorber for attenuating forearm tremor. Med Bio Eng Comput 56(5):923–930
5. Rocon EJ, Belda-Lois MA, Ruiz F, Manto M, Moreno JC, Pons JL (2007) Design and validation of a rehabilitation robotic exoskeleton for tremor assessment and suppression. IEEE Trans Neural Syst Rehabil Eng 15(3):367–378
6. Kotovsky J, Rosen M (1998) A wearable tremor-suppression orthosis. J Rehabil Res Dev 35(4):373–387
7. Hashemi SM, Golnaraghi MF, Patla AE (2004) Tuned vibration absorber for suppression of rest tremor in Parkinson's disease. Med Bio Eng Comput 42(1):61–70
8. Gebai S, Hammoud M, Khachfe H (2018) Parametric study of an enhanced passive absorber used for tremor suppression. Struct Control Health 25(7):e2177
9. Gebai S, Hammoud M, Hallal A, Al Shaer A (2018) Structural control and biomechanical tremor suppression: comparison between different types of passive absorber. J Vib Control 24(12):2576–2590
10. López-Blanco R, Velasco MA, Méndez-Guerrero A, Romero JP, del Castillo MD, Serrano JI, Rocon E, Benito-León J (2019) Smartwatch for the analysis of rest tremor in patients with Parkinson's disease. J Neurol Sci 401:37–42
11. Habib G, Detroux T, Viguié R, Kerschen G (2015) Nonlinear generalization of Den Hartog's equal-peak method. Mech Syst Signal Process 52:17–28
12. Mohanty S, Dwivedy SK (2019) Nonlinear dynamics of piezoelectric-based active nonlinear vibration absorber using time delay acceleration feedback. Nonlinear Dyn 98(2):1465–1490
13. Mohanty S, Dwivedy SK (2019) Active nonlinear vibration absorber for a nonlinear system with a time delay acceleration feedback under the internal resonance, subharmonic, superharmonic and principal parametric resonance conditions simultaneously. J Aerospace Syst Eng 13(5):9–15
14. Mohanty S, Dwivedy SK (2017) Dynamic analysis of active vibration absorber by time delay acceleration feedback using higher order method of multiple scales. In: ASME gas turbine India conference 58516, pp. V002T05A033-43
15. Mohanty S, Dwivedy SK (2019) Active vibration absorber for a nonlinear system with time-delay acceleration feedback for superharmonic and subharmonic resonance conditions. In: Machines, mechanism and robotics. Springer, Singapore, pp 681–690
16. Mohanty S, Dwivedy SK (2020) Active nonlinear vibration absorber for a harmonically excited beam system. In: Nonlinear dynamics control. Springer, Cham, pp 3–11